12-8-1972

Elastic-Plastic Poisson's Ratio of Borsic-Reinforced Aluminium Composites

Ronald Edward Allred

ELASTIC - PLASTIC - ALLRED

THE UNIVERSITY OF NEW MEXICO
ALBUQUERQUE, NEW MEXICO 87106

Policy on Use of Theses and Dissertations

Unpublished theses and dissertations accepted for master's and doctor's degrees and deposited in the University of New Mexico Library are open to the public for inspection and reference work. *They are to be used only with due regard to the rights of the authors.* The work of other authors should always be given full credit. Avoid quoting in amounts, over and beyond scholarly needs, such as might impair or destroy the property rights and financial benefits of another author.

To afford reasonable safeguards to authors, and consistent with the above principles, anyone quoting from theses and dissertations must observe the following conditions:

1. Direct quotations during the first two years after completion may be made only with the written permission of the author.

2. After a lapse of two years, theses and dissertations may be quoted without specific prior permission in works of original scholarship provided appropriate credit is given in the case of each quotation.

3. Quotations that are complete units in themselves (e.g., complete chapters or sections) in whatever form they may be reproduced and quotations of whatever length presented as primary material for their own sake (as in anthologies or books of readings) ALWAYS require consent of the authors.

4. The quoting author is responsible for determining "fair use" of material he uses.

This thesis/dissertation by Ronald Edward Allred has been used by the following persons whose signatures attest their acceptance of the above conditions. (A library which borrows this thesis/dissertation for use by its patrons is expected to secure the signature of each user.)

NAME AND ADDRESS	DATE

July 1971—1,000—GS

This thesis, directed and approved by the candidate's committee, has been accepted by the Graduate Committee of The University of New Mexico in partial fulfillment of the requirements for the degree of

MASTER OF SCIENCE

ELASTIC-PLASTIC POISSON'S RATIO OF BORSIC-
Title REINFORCED ALUMINUM COMPOSITES

RONALD EDWARD ALLRED
Candidate

NUCLEAR ENGINEERING
Department

Wayne P. Moellenberg
Dean

December 8, 1972
Date

Committee

James A. Horak
Chairman

Howard L. Schreyer

David W. Schuster

ELASTIC-PLASTIC POISSON'S RATIO OF BORSIC-REINFORCED ALUMINUM COMPOSITES

BY

RONALD EDWARD ALLRED

B.S., University of New Mexico, 1968

THESIS

Submitted in Partial Fulfillment of the

Requirements for the Degree of

Master of Science in Materials Science and Engineering

in the Graduate School of

The University of New Mexico

Albuquerque, New Mexico

December, 1972

Acknowledgments

The inspiration, instruction and untiring efforts in the behalf of Materials Science students of Professor James A. Horak is gratefully acknowledged. The author is especially grateful to Dr. William R. Hoover and Dr. H. L. Schreyer for guidance throughout the course of this study.

The author would like to thank Dr. David M. Schuster and other members of the Composite Materials Development Division at Sandia Laboratories for their support and assistance. The aid of Mary Wood in the preparation of the manuscript is also gratefully appreciated.

A special appreciation is given to the author's wife, Katherine Jenison, who has given infinite understanding and encouragement during the course of this study.

Finally, the author gratefully acknowledges the financial support of Sandia Laboratories.

ELASTIC-PLASTIC POISSON'S RATIO OF BORSIC-REINFORCED ALUMINUM COMPOSITES

BY

Ronald Edward Allred

ABSTRACT OF THESIS

Submitted in Partial Fulfillment of the

Requirements for the Degree of

Master of Science in Materials Science and Engineering

in the Graduate School of

The University of New Mexico

Albuquerque, New Mexico

December, 1972

ABSTRACT

Poisson's ratio as a function of tensile strain has been examined for four volume fractions of unidirectional Borsic-reinforced aluminum composites. Linear relationships were found between Poisson's ratio and fiber volume fraction during Stage I (elastic filaments-elastic matrix) and Stage II (elastic filaments-plastic matrix) deformation which confirms that rule-of-mixtures equations may be used to predict Poisson's ratios for metal-matrix composites. These equations must be used with care, however, due to differences in the Poisson's ratio behavior of the components of the composite when tested alone and *in situ* in the composite. These differences are attributed to the triaxial stress field generated in the composite during deformation.

Table of Contents

List of Figures

List of Tables

Abbreviations and Symbols

cfh = cubic feet per hour

DY = array of error estimates

e^p = increment of plastic strain

F = yield function

I_1^2 = $(\sigma_1 + \sigma_2 + \sigma_3)^2$

k = transverse gage sensitivity

ksi = thousands of pounds per square inch

n = number of data values

N.D. = not detected

R = array of smooth spline values

psi = pounds per square inch

V_f = volume fraction of filament

V_m = volume fraction of matrix

v/o = volume percent

Y = ordinate array

Y_1 = uniaxial yield stress

α = constant which is a measure of the permanent volumetric deformation

ϵ = strain

ϵ_{ult} = failure strain

$\Delta\lambda$ = scalar function relating the effective increment in strain to the effective stress

σ = stress

σ_{ult} = ultimate tensile stress

ν = Poisson's ratio

ν_f = Poisson's ratio of filament

ν_m = Poisson's ratio of matrix

$\nu_{m|_\epsilon}$ = Poisson's ratio of unreinforced matrix at composite strain

Introduction

Recent demands for materials of high strength and stiffness and low weight for use in aerospace applications have prompted the development of metal composites reinforced with high strength fibers. The consideration of fiber-reinforced, metal-matrix composites for use in engineering structures has motivated the determination of the mechanical properties of these materials for design purposes. The need for accurate experimental mechanical property data is further increased by the anisotropy of mechanical and physical properties inherent to these composites which complicates theoretical analysis of their deformation behavior.

Of the material parameters used to describe the deformation process, the lateral contraction or Poisson's ratio has received little attention in the case of fiber-reinforced metal-matrix composite materials. For unidirectionally reinforced composites, Poisson's ratio, ν, may be defined in terms of principal strains as:

$$\nu_{13} = \frac{\epsilon_1}{\epsilon_3} = \frac{\epsilon_2}{\epsilon_3} = \nu_{23} \qquad (1)$$

where

$\nu_{13} = \nu_{23}$ = Poisson's ratio

ϵ_3 = longitudinal strain in the direction of an applied tensile force parallel to the filament direction

$\epsilon_1 = \epsilon_2$ = transverse strain acting in directions orthogonal to the applied tensile force and the filaments

Poisson's ratio for isotropic materials is an elastic constant related to the material elastic moduli. Theoretically, ν cannot vary in the range over which Hooke's law applies (i.e., the elastic range), however, a decrease in Poisson's ratio prior to the nominal yield stress has been reported and attributed to the beginning of plastic deformation.[1] With the onset of plastic deformation Poisson's ratio ceases to remain a material elastic constant but may still be regarded as a ratio of transverse and longitudinal strains in accord with Equation (1). Typically, Poisson's ratio for isotropic materials in the plastic deformation range increases to a value near 0.5 with increasing plastic strain, levels off, and then drops.[1] The critical value of 0.5 corresponds to the limiting case of material incompressibility and characterizes a material which offers no resistamce to change of shape and for which Young's modulus and the torsion modulus are zero.[1] The transition from ν as an elasticity characteristic to the limiting plastic value is viewed as plastic flow of microvolumes which increase in volume until a fully plastic state is achieved.[2]

In contrast to the behavior of homogemeous metals, for anisotropic fiber reinforced materials in which the filaments are continuous, uniformly distributed and aligned in the

direction of load, deformation occurs in four states.[3,4,5] The stages of deformation observed are:

(I) Filaments and matrix deform elastically.

(II) Filaments deform elastically and matrix deforms plastically.

(III) Both phases deform plastically.

(IV) Filament failure followed by composite failure.

Throughout the entire range of deformation composite properties are often estimated by combining the properties of the constituent phases. The most familiar of these relations is the rule of mixtures in which the relative contribution of each phase is calculated as a function of volume fraction.[3,4,6]

The major Poisson's ratio, ν_{13}, for a unidirectional fiber-reinforced composite loaded parallel to the filament direction has been predicted to follow a rule of mixtures behavior in the elastic range[7,8,9] which may be represented as:

$$\nu_{13} = \nu_f V_f + \nu_m(1 - V_f) \qquad (2)$$

where

ν_{13} = major Poisson's ratio

ν_f = fiber Poisson's ratio

ν_m = matrix Poisson's ratio

V_f = fiber volume fraction.

Thus, if Poisson's ratio of each of the components is known, the elastic Poisson's ratio of the composite may be predicted

by Equation (2). Equation (2) has been verified experimentally in epoxy based systems;[10,11] and, although not proven directly in metal matrix composites several investigators have reported a linear relationship between ν_{13} and fiber volume fraction.[12,13,14]

The majority of reinforcing fibers with high specific strength and stiffness are also brittle, i.e., they exhibit little or no plastic deformation prior to failure. A metal composite reinforced with brittle fibers of this type will not undergo the Stage III deformation listed previously, rather the major portion of the stress versus strain curve for such a composite is Stage II deformation with Stage I ending at low strain levels.

A thorough understanding of Stage II deformation is of prime importance in practical metal-matrix composites because efficient design and application dictates use of these materials with the matrix in a yielded condition. Consequently, Poisson's ratio during Stage II deformation is a basic design parameter of fiber-reinforced metal composites.

Since the reinforcing phase remains elastic to failure, the asymptotic value of ν for such a composite will be less than the critical value of 0.5 observed in homogeneous isotropic metals. Little theoretical work has been done on the prediction of plastic range Poisson's ratios for composites. Except for a recent analysis based on the stress versus strain

curve of the composite,[15] a modified rule of mixtures approach is generally utilized to predict plastic range Poisson's ratios of composites.[16] This relation is given in Equation (3):

$$\nu_{13} = \nu_f V_f + \nu_m\Big|_{\epsilon} (1 - V_f) \qquad (3)$$

where

$\nu_m\Big|_{\epsilon}$ = Poisson's ratio of the matrix alone at the composite strain

To this author's knowledge, there are no experimental values of Stage II Poisson's ratio in the literature and thus no verification of Equation (3) has been obtained.

The most highly developed metal-matrix composite system of practical use for structural applications at this time is boron or Borsic* reinforced aluminum. The B-Al composite system has a high strength and stiffness to weight ratio and may be fabricated relatively easily by conventional plasma-spraying and hot-pressing methods. Because B-Al is being applied to structural applications at the present time, it is appropriate to more fully characterize its deformation behavior.

It is the purpose of the present work to experimentally

*Borsic is the registered trade name of the silicon carbide coated boron filaments made by Hamilton-Standard division of United Aircraft Corporation.

determine Poisson's ratio of continuous, unidirectional Borsic reinforced aluminum composites as a function of strain and filament volume fraction. The results of this study will, in addition to providing experimental values of Poisson's ratio for design purposes, determine the applicability of rule of mixtures predictions for elastic (Equation (2)) and elastic-plastic (Equation (3)) Poisson's ratios in metal-matrix composites.

Experimental Procedure

Sample Preparation

Composite plates of unidirectional Borsic filaments in an 1100 aluminum alloy matrix were fabricated by a modification of the monolayer tape method employed commercially by Hamilton-Standard.[17,18] The monolayer tape method consisted of winding 4.2 mil diameter Borsic filament around a smooth steel mandrel with a filament winding lathe. The wrapped mandrel was then mounted in a plasma-spraying hood and rotated while a surface coating of 1100 aluminum was applied by plasma-spraying with the conditions given in Table 1. Four volume fractions of Borsic filament were manufactured by changing the filament center-to-center spacing and the thickness of the plasma-sprayed aluminum coating.

The Borsic-aluminum tape was cut along the axis of the mandrel and removed as a sheet approximately 1.5 feet by 2.0 feet. Because of the high modulus of the Borsic filaments (55-60 x 10^6 psi) the sheet lay flat after removal from the mandrel. These sheets were then cut with a paper cutter to dimensions of 2.25 inches x 3.5 inches and ultrasonically cleaned in acetone. After drying the sections were

stacked in groups of 25 with the filaments unidirectionally aligned. The stacks were then wrapped with 5 mil thick 1100 aluminum foil to help maintain the plate geometry and placed in stainless steel bags to minimize oxidation during the subsequent diffusion bonding operation.

Samples, in the stainless steel bags, were then hot pressed between flat rams for 5 minutes at 540°C and 10,000 psi. The bags containing the pressed plates were removed from the press and slow cooled in air. Plate thicknesses varied from 0.118 inches to 0.251 inches.

Representative cross sections from each plate were mounted in epoxy and polished metallographically. Sample cross sections exhibiting typical filament distributions for each volume fraction are shown in Figures 1-4.

Plates of unreinforced plasma-sprayed 1100 aluminum were prepared in addition to the composite specimens. To make these plates, a 0.250 inch thick deposit of aluminum was plasma-sprayed onto a rotating hexagonal aluminum mandrel. The spraying parameters used were identical to those used in manufacturing the composite monolayer tapes (Table 1).

The 1100 aluminum alloy was chemically analyzed at Sandia Laboratories for impurity content in the as-received powder and plasma-sprayed conditions. The oxygen content was determined by neutron activation analysis. Analytical results of the impurity content of the 1100 aluminum powder

and plasma-sprayed 1100 aluminum are given in Table 2.

To remove the porosity inherent to the plasma-spraying process, flat sections 2.25 inches x 3.5 inches were machined out of the plasma-sprayed aluminum tube, sealed in stainless steel bags and hot-pressed under the same conditions used for the composite plates. Polished cross sections of the densified plasma-sprayed aluminum are shown in Figures 5 and 6.

The surface layer of aluminum was removed from the composite plates by grinding to prevent any anomalous surface behavior from affecting test results. Tensile specimens 0.345 inches wide by 3.5 inches long were then ground from the composite plates parallel to the filament direction. Specimens of the densified plasma-sprayed aluminum were machined into subsize rectangular tensile bars with a one inch reduced gage section similar to ASTM specification No. E-8.[19]

Testing Equipment and Procedure

One inch wide aluminum tabs were epoxied on the specimen ends with the aid of a centering jig. The tabs were employed to ensure uniform load application across the specimen ends and to provide ease of alignment in the Instron wedge action grips since specimen alignment has been shown to be a critical factor in obtaining valid

Poisson's ratio data from composites.[20]

Standard foil type SR-4 biaxial strain gages as manufactured by BLH Electronics, Inc. were mounted on both sides of the specimens with epoxy prior to testing. The samples were then pulled in tension on an Instron testing machine at a crosshead rate of 0.008 inches per minute. Load was monitored on the Instron X-Y recorder and the strain recorded on a B and F Instruments, Inc. model 161 multichannel digital strain indicator. In addition, a set of the densified unreinforced plasma-sprayed aluminum specimens were tested with a one inch strain gage extensiometer to obtain the entire stress-strain curve.

Due to the difference in thermal expansion between the component phases, composites are subjected to a state of residual stress upon cooling from an elevated temperature. For this reason, all samples were preloaded to approximately 5 percent of their ultimate strength and unloaded to stabilize the residual stress state of the composite and seat the strain gages.[21] The load-unload cycle was repeated three times at which time the stress versus strain hysteresis loop became completely closed. Samples were then loaded to failure with strain being monitored at even load increments. Failure of the composite samples occurred almost exclusively in or near the grip sections which is a common problem in the testing of composites at this time. However, due to the large distance

between the strain gages and any stress concentration present in the grip sections it is believed that the strain readings obtained are valid.

In order to compensate for any possible bending of the specimen the average transverse and axial strains were obtained by averaging the respective transverse and axial strains of the two gages. Poisson's ratio was calculated at each load increment by the transverse gage correction method of Baumberger and Hines.[22] The correction which includes the effect of Poisson's ratio of the strain gage may be represented as:

$$\nu_{13} = (\epsilon_1/\epsilon_3 - k)/(1 - k\,(\epsilon_1/\epsilon_3)) \qquad (3)$$

where

ν_{13} = major Poisson's ratio

ϵ_3 = axial strain

ϵ_1 = transverse strain

k = transverse gage sensitivity

Filament volume fractions were determined by dissolving the aluminum matrix in 6N NaOH at 66°C and filtering the undissolved Borsic filaments into weighed filtering crucibles. In this manner, the weight percent Borsic was determined which is equal to volume percent Borsic due to the equal densities of Borsic and aluminum. Filament volume fractions used in this study were determined to be 13.1, 34.2, 40.9 and 53.9 percent Borsic.

Results

To gain insight into composite deformation behavior it is helpful to understand the behavior of the constituent phases. It is well established that Borsic filaments remain elastic to failure while exhibiting a modulus of 55-60 x 10^6 psi.[23] The deformation behavior of the plasma-sprayed 1100 aluminum is not well documented; therefore, its behavior was experimentally determined in this study. Typical stress versus strain and Poisson's ratio versus strain curves for the unreinforced densified plasma-sprayed aluminum were determined through a series of tensile tests and are given in Figures 7 and 8.

Poisson's ratios of the densified plasma-sprayed aluminum were calculated as a function of axial strain to a strain of 1 percent where the biaxial strain gages failed. A best fit plot of the Poisson's ratio data is also shown in Figure 8 as determined by averaging the data for strains less than 0.05 percent and fitting a smoothing spline to the balance of the curve. The smoothing spline (subroutine SMØØTH[24]) minimized the integral of the second derivative subject to the constraint that:

$$\sum_{I=1}^{n} \left[\frac{R(I) - Y(I)}{DY(I)}\right]^2 \leq n \qquad (4)$$

where

R = array of smooth spline values

Y = ordinate array

DY = array of error estimates (actually standard deviation in Y(I))

n = number of data values

Error estimates for these and subsequent data sets were varied for each data set until a best fit curve was obtained.

With the behavior of the matrix material documented, the stress versus strain response of the Borsic-reinforced aluminum composites was determined. The typical stress versus strain curve for the composite (Figure 9) may be divided into two regions which are characteristic of brittle-fiber-reinforced composite materials.[3,4,5] The initial linear region (Stage I) reflects the elastic response of both filaments and matrix while the nonlinear region (Stage II) is characteristic of composite response when the filaments are elastic and the matrix is plastic. It may be seen that because of the gradual transition from linear to nonlinear behavior the stress level at which the matrix yields is difficult to define using a composite stress versus strain curve.

The Poisson's ratios calculated for the four volume fractions examined in this study are plotted as a function of axial strain in Figures 10-13. As was calculated for the unreinforced aluminum, best fit curves to the data were

determined using the program SMØØTH[24] and are also plotted in Figures 10-13. The shape of these ν versus ϵ curves is similar for all four volume fractions. The data indicates that changes in volume fraction change only the relative magnitude of the measured Poisson's ratios.

In order to summarize the data presented in Figures 7-13, average values of the elastic and asymptotic plastic Poisson's ratios and the elastic moduli were calculated and are given in Table 3.

Discussion

Densified Plasma-Sprayed Aluminum

The mechanical behavior of unreinforced hot-pressed plasma-sprayed aluminum was determined in this study since it differs considerably from wrought aluminum. Because of its oxide content it would be expected that plasma-sprayed aluminum would exhibit property trends similar to those of dispersion strengthened aluminum alloys (SAP).[25] Typical trends shown by SAP alloys are higher yield and ultimate strengths and lower ductility,[26] all of which may be explained by the interaction of dislocations with the dispersed oxide particles.[27] Handbook values[28] of yield and ultimate strengths and elongation for 1100-0 aluminum (hereafter referred to as aluminum) are compared with the experimental results for densified plasma-sprayed aluminum in Table 4. The results obtained for plasma-sprayed 1100 aluminum are in agreement with those obtained by other investigators.[29] It is seen that nominal handbook values for 1100 aluminum are not representative of the densified plasma-sprayed aluminum matrix used for the composites in this study.

Since compacted plasma-sprayed aluminum behaves differently than wrought aluminum when undergoing plastic deformation, it would be expected that the plastic Poisson's

ratio of densified sprayed aluminum would also deviate from that exhibited by wrought aluminum. In the elastic range, however, ν should agree for both materials since ν, as an elasticity characteristic, belongs to the class of mechanical parameters that are practically insensitive to structural changes.[2] As seen in Figure 8, this is observed in the current study since the elastic Poisson's ratio of 0.33 for compressed sprayed aluminum agrees exactly with that of 0.33 for wrought aluminum.[30]

With the onset of plasticity, however, a wide divergence between ν of the sprayed aluminum and wrought aluminum occurs. A comparison of Poisson's ratios at 1 percent axial strain shows that ν for plasma-sprayed aluminum is approximately 0.365 (Figure 8), whereas ν for wrought aluminum is near 0.45.[30] The reduced value of ν in the oxide dispersion strengthened material may be predicted by assuming that a finite amount of permanent volumetric deformation can occur in the plastic range.[31]

Compressible plastic volumetric deformation may be theoretically considered by defining the yield function, F, such that it depends upon the first invariant of the stress deviator as well as the second:

$$F(\alpha,\sigma_1) \equiv \bar{\sigma}^2 + \alpha I_1^2 - (1 - \alpha)Y_1^2 = 0 \qquad (5)$$

where

$\bar{\sigma}$ = effective stress in the sample

$= 1/2\left[(\sigma_1 - \sigma_2)^2 + (\sigma_2 - \sigma_3)^2 + (\sigma_1 - \sigma_3)^2\right]^{1/2}$

Y_1 = uniaxial yield stress

$I_1^2 = (\sigma_1 + \sigma_2 + \sigma_3)^2$

α = a constant which is a measure of the permanent volumetric deformation

With loading from zero stress, the yield function is initially negative. Plastic deformation begins when F = 0 and with additional loading each increment of plastic strain is given by the flow rule:[32]

$$\Delta e_i^p = \Delta\lambda \frac{\partial F}{\partial \sigma_i} \tag{6}$$

where $\Delta\lambda$ = scalar function relating the effective increment in strain to the effective stress

Equation (6) may be expanded to Equations (7) for clarity.

$$\Delta e_1^p = \Delta\lambda \left[2\sigma_1 - \sigma_2 - \sigma_3 + 2\alpha(\sigma_1 + \sigma_2 + \sigma_3)\right] \tag{7a}$$

$$\Delta e_2^p = \Delta\lambda \left[2\sigma_2 - \sigma_1 - \sigma_3 + 2\alpha(\sigma_1 + \sigma_2 + \sigma_3)\right] \tag{7b}$$

$$\Delta e_3^p = \Delta\lambda \left[2\sigma_3 - \sigma_1 - \sigma_2 + 2\alpha(\sigma_1 + \sigma_2 + \sigma_3)\right] \tag{7c}$$

For large strains (i.e. well into the plastic region), Poisson's ratio can be estimated as:

$$\nu_{13} = \frac{-\Delta e_1^p}{\Delta e_3^p} = \frac{-\left[2\sigma_1 - \sigma_2 - \sigma_3 + 2\alpha(\sigma_1 + \sigma_2 + \sigma_3)\right]}{\left[2\sigma_3 - \sigma_1 - \sigma_2 + 2\alpha(\sigma_1 + \sigma_2 + \sigma_3)\right]} \tag{8}$$

The state of stress for the densified plasma-sprayed aluminum is uniaxial, i.e., $\sigma_1 = \sigma_2 = 0$. For this case, Equation (8) reduces to:

$$\nu_{13} = 1/2 \frac{(1-2\alpha)}{(1+\alpha)} \tag{9}$$

For the case of an ideally plastic material $\alpha = 0$ and ν_{13} reduces to the critical value of 1/2. At 0.4 percent strain Poisson's ratio for the compressed sprayed aluminum is 0.352 (Figure 8), which corresponds to a value of $\alpha = 0.107$. This represents a volumetric change of 0.136 percent. Such a volume change may be reasonably attributed to porosity generated by dislocation-oxide particle interactions, fracturing of the particle-matrix interface and/or fracture of the oxide particles themselves.

In summary, the mechanical behavior of densified plasma-sprayed aluminum shows property trends similar to SAP alloys and is not similar to wrought aluminum. The elastic Poisson's ratio of hot-pressed sprayed aluminum is 0.33 which is identical to that of wrought aluminum. In the plastic range, however, Poisson's ratio of the compacted sprayed aluminum differs from that of wrought aluminum due to the oxide particles present in the sprayed aluminum. With this understanding of the constituent phases, it is mow appropriate to examine their behavior combined into a composite.

Elastic Composite Behavior

The behavior of Poisson's ratio in Borsic-filament-reinforced aluminum composite materials may be most conveniently discussed by examining the shape of the ν versus ϵ curves plotted in Figures 10-13. The general shape of the curves is the same for all filament volume fractions. For purposes of discussion, the composite ν versus ϵ curves may be divided into three distinct regions: (1) Region I for ϵ less than 0.05 percent, (2) Region II for the transition region of ϵ between 0.05 and 0.20 percent and (3) Region III for ϵ greater than 0.20 percent.

Region I is characterized by the elastic response of both the filaments and matrix and corresponds to Stage I of the composite stress versus strain curve. To gain insight into filament and matrix behavior in Region I, the average elastic Poisson's ratios for each volume fraction are plotted as a function of volume fraction in Figure 14. The data of Figure 14 may be reasonably described by a least squares fit because all the data lies within 5 percent of the line. The *in situ* elastic Poisson's ratio behavior of the filaments and matrix may be determined by extrapolating the least squares line to the end points.

At a filament volume fraction of zero, which corresponds to the matrix behavior, a ν of 0.33 is obtained by this method. This value is in excellent agreement with the measured result

of 0.33 for the matrix alone (Table 3). Extrapolating to one hundred volume percent Borsic yields ν of the filaments equal to 0.15. This value is somewhat lower than the value of 0.20 currently in use in the literature for Borsic.[33] It should be noted however, that experimental measurements of Poisson's ratio for thin filaments are rarely reported in the literature. More often, Poisson's ratios are calculated by using the simple elasticity relationship between Young's modulus and the shear modulus which are subject to experimental variations.[34]

The observation that ν is a linear function of filament content in the elastic range (Figure 14) indicates that it can be successfully predicted by a rule of mixtures approach such as Equation (2). However, a filament Poisson's ratio of 0.15, which is lower than that generally assumed, must be used in conjunction with the accepted aluminum value of 0.33 to obtain agreement with the experimental results.

Inelastic Composite Behavior

The transition region (Region II) of the composite Poisson's ratio versus strain curve may be viewed as a gradual transition from an elastic to a fully plastic matrix. Comparison of the slope of the composite transition region in Figures 10-13 with that of the densified plasma-sprayed aluminum transition (Figure 8) shows the composite

slope to be much steeper than that of the matrix material. The increased rate of change of the composite curve indicates that regions of nonhomogeneous plastic deformation in the composite are enlarging faster than similar regions in the densified plasma-sprayed aluminum alone.[35] This difference in behavior may be accounted for by the complex stress distribution acting on the composite matrix.

Unlike the homogeneous aluminum specimens stressed in uniaxial tension, stresses out of the loading plane are generated in the composite matrix due to the difference in Poisson's ratios between the constituent phases in the composite. The resultant stress state has been the object of numerous theoretical and experimental studies.[34,36-43] A general conclusion from these studies is that the matrix in a composite reinforced with filaments of higher modulus and lower Poisson's ratio experiences radial compression and circumferential tension when subjected to a uniaxial load. It has also been concluded that the highest compressive stresses on the composite matrix occur at the filament-matrix interface.

Based upon these prior observations the increased slope of the composite curve in Region II may be interpreted as local yielding beginning in the matrix at the filament-matrix interface. With additional loading, additional yielding occurs and the plastic region spreads rapidly

through the matrix. An additional complicating factor is provided by the increase in the matrix Poisson's ratio upon yielding. As the matrix Poisson's ratio increases the mismatch in Poisson's ratios between the filaments and matrix increases which magnifies the induced transverse stress field.

Attempts to determine the rate-of-change of the composite ν versus ϵ curves given in Figures 10-13 as a function of the fiber volume fraction were unsuccessful because of the range of sensitivity of the experiment conducted. An increasing rate of plasticity should be present with increasing filament volume fraction if the proposed mechanism is correct. As the filament volume fraction increases, the filament spacing decreases. A plastic region at the filament-matrix interface would thus have to traverse a shorter distance to meet another plastic region. The result would be a higher rate of change of plasticity in the higher volume fraction composites.

The abrupt change in slope of the composite ν versus ϵ curve at a strain of approximately 0.05 percent may be used to provide valuable information on the nature of the matrix behavior. Conventional methods of determining yield in metal-matrix composite materials are inadequate due to the gradual change in slope of the composite stress versus strain curve between Stage I and Stage II deformation as seen in Figure 9. The abrupt change in the ν versus ϵ curve with

the onset of plasticity provides a very accurate means for the determination of matrix yield.

Following the transition region between longitudinal strains of 0.05 and 0.20 percent, the ν versus ϵ curve is characterized by an asymptotic value. The asymptotic value in Region III in the case of a brittle fiber-reinforced metal composite is not near 0.5 as in an isotropic homogeneous metal. Rather, one observes a combination of the Poisson's ratios of the constituent phases. The experimental values of the composite plastic Poisson's ratio in Region III (longitudinal strains greater than 0.20 percent) corresponding to composite Stage II deformation were averaged and are plotted versus fiber volume fraction in Figure 15. The data of Figure 15 may be adequately described by the least squares fit shown as all the data lie within 10 percent of the least squares line.

The observation that ν is a linear function of volume fraction in Stage II is of considerable engineering importance. This means that the Poisson's ratio of a composite system in which the matrix is plastic may be predicted by a simple relation such as Equation (3).

To determine the component values necessary to predict the experimental data the line in Figure 15 must be extrapolated to obtain the <u>in situ</u> behavior of the constituent phases in Stage II. At one hundred percent Borsic a Poisson's

ratio of 0.15 is obtained from the plastic range data. This value is the same as the filament elastic range value reported earlier. Since Borsic filaments remain elastic to failure, Poisson's ratio of the filaments should remain constant to failure. The agreement between ν of the filaments in Stage I and Stage II lends further credence to the experimental methods employed in this investigation.

Examining Figure 15 at a filament volume fraction of zero results in a value of 0.40 for the in situ matrix Poisson's ratio. Examination of the Poisson's ratio data for the matrix alone (Figure 8) at similar strains shows no agreement with the in situ result. The composite matrix ν of 0.40 is much greater than that shown by the densified plasma-sprayed aluminum of 0.355. The in situ result is also much higher than that of what appears to be the asymptote of the ν versus ϵ curve for the aluminum alone at 0.365 which occurs at much larger strains. The higher value of ν of the composite matrix indicates that the aluminum in the composite is behaving more plastically than it would without the filaments present.

As mentioned previously, the stress field in the composite is not uniaxial because transverse stresses are generated due to the mismatch in Poisson's ratio between the filaments and matrix. Equation (8) may be used to approximate the stress distribution necessary to theoretically

explain the experimental results. In the composite σ_1 and σ_2 are not zero which necessitates making some approximations to facilitate their calculation.

Consider a typical point in the matrix in the interior of the composite to eliminate surface effects. It may be assumed that the transverse stresses have no directional dependence, i.e., $\sigma_1 = \sigma_2$. Solving Equation (8) for $\nu_{13} = 0.40$ and $\sigma_1 = \sigma_2$ results in an estimation of σ_1 or σ_2 equal to $-0.125\ \sigma_3$.

The prediction that the summation of σ_1 and σ_2 is a compressive stress is at variance to current micromechanics analyses in the literature.[34,36-43] A general result of these analyses is that the tensile circumferential stress is larger in magnitude than the compressive radial component which results in a tensile resultant stress. The apparent anomaly between current theory and this experimental work cannot be resolved at this time. However, current micromechanics analyses do not allow for permanent volumetric deformation. It is possible that a more refined analysis considering permanent volumetric deformation would bring theoretical and experimental results into better agreement.

The experimental data show the aluminum matrix of the composite to be more plastic than homogeneous aluminum at comparable strains. This indicates that use of Equation (3) to predict composite plastic Poisson's ratios must be done

with care. At this time, the matrix plastic Poisson's ratio must be experimentally determined since analysis is unable to predict it.

Conclusions

The results of this study of Poisson's ratio for Borsic-reinforced aluminum composites suggest the following conclusions:

1. The linear relationship between Poisson's ratio and filament volume fraction for Stage I and Stage II deformation confirms that rule of mixtures calculations may be used to predict elastic and plastic composite Poisson's ratios.
2. The *in situ* value of Poisson's ratio for Borsic filaments is 0.15.
3. Unreinforced densified plasma-sprayed aluminum under uniaxial stress shows a decreased value (0.355) of plastic Poisson's ratio compared to wrought aluminum (0.450).
4. The elastic Poisson's ratio of the plasma-sprayed aluminum composite matrix, measured *in situ*, is 0.33 which agrees with that of the plasma-sprayed aluminum matrix alone.
5. The plastic Poisson's ratio of the aluminum composite matrix, measured *in situ*, is 0.40. This value is higher than the aluminum matrix alone. The difference is attributed to the triaxial stress state on the composite matrix.

6. The abrupt change in slope of the Poisson's ratio versus longitudinal strain curve upon matrix yield may be used as an accurate method of determining matrix yield in filament-reinforced, metal-matrix composites.

Bibliography

1. W. Köster and H. Franz, "Poisson's Ratio for Metals and Alloys," Met. Revs., 6, 21, 1961, p. 1.

2. V. A. Kuz'menko, "Regularities in the Variation of Transverse Strain Coefficients," Institute of Strength Problems at the Academy of Sciences of the Ukranian SSR, Kiev, translated from Problemy Prochnosti, No. 8, August 1971, p. 48.

3. D. L. McDaniels, R. W. Jech and J. W. Weeton, "Analysis of Stress-Strain Behavior of Tungsten-Fiber Reinforced Copper Composites," Trans. Met. Soc. AIME, 233, 1965, p.636.

4. A. Kelly and G. J. Davies, "The Principals of the Fiber Reinforcement of Metals," Met. Revs., 10, 37, 1965, p. 1.

5. A. Kelly and H. Lilholt, "Stress-Strain Curve of a Fiber-Reinforced Composite," Phil. Mag., 19, 1969, p. 311.

6. A. A. Baker and D. Cratchley, "Stress-Strain Behavior and Toughness of a Fiber-Reinforced Metal," App. Mat'ls Res., 5, 1966, p. 52.

7. J. Ekvall, "Elastic Properties of Orthotropic Monofilament Laminates," Paper 61-Av-5, Amer. Soc. Mech. Engrs., March 1961.

8. D. Abolin'sh, "Compliance Tensor for an Elastic Material Reinforced in One Direction," Polymer Mechanics, 1, 4, 1965, p. 28.

9. J. C. Halpin and S. W. Tsai, "Environmental Factors in Composite Materials Design," AFML-TR-67-423, Air Force Materials Laboratory, Wright-Patterson AFB, 1967.

10. J. E. Ashton, J. C. Halpin and P. H. Petit, Primer on Composite Materials: Analysis, Technomic Pub. Co., Stamford, Conn., 1969.

11. S. W. Tsai, "Structural Behavior of Composite Materials," NASA-CR-71, National Aeronautics and Space Administration, 1964.

12. J. R. Long, "The Evaluation of the Mechanical Behavior of Metal Matrix Composites Reinforced with SiC-Coated

Boron Fibers," AFML-TR-69-291, Vol. I, Air Force Materials Laboratory, Wright-Patterson AFB, 1969.

13. E. M. Lenoe, R. P. Murro, S. Beaumont and J. Wu, "Micromechanics of High Strength, Low Density, Boron Filament Reinforced Metallic Composites," AFML-TR-67-125, Vol. II, Air Force Materials Laboratory, Wright-Patterson AFB, 1967.

14. W. H. Schaefer and J. L. Christian, "Evaluation of the Structural Behavior of Filament Reinforced Metal Matrix Composites," AFML-TR-69-36, Vol. III, Air Force Materials Laboratory, Wright-Patterson AFB, 1969.

15. C. W. Bert, "Plasticity and Creep Analysis of Filamentary Metal-Matrix Composites," SC-DR-720055, Sandia Laboratories, Albuquerque, New Mexico, 1972.

16. C. T. Lynch and J. P. Kershaw, Metal Matrix Composites, CRC Press, Cleveland, 1972, p. 134.

17. "Borsical Tape and Broad Goods," Hamilton-Standard, Technical Data Sheet No. HSCM-3-K, Windsor Locks, Conn., 1971.

18. "Borsic-Aluminum Composites," Hamilton-Standard, Technical Data Sheet No. HSCM-4-B, Windsor Locks, Conn., 1969.

19. "Standard Methods of Tension Testing of Metallic Materials," ASTM Standards, Part 31, Designation: E8-68, American Society for Testing and Materials, 1969, p. 205.

20. J. M. Slepetz, "Elastic Characterization of Fiber Reinforced Composites," Composite Materials, Advisory Group for Aerospace Research and Development Conference, paper 10, 1970.

21. D. Cratchley, A. A. Baker and P. W. Jackson, "Mechanical Behavior of a Fiber Reinforced Metal and Its Effect Upon Engineering Applications," Metal Matrix Composites, ASTM STP 438, American Society for Testing and Materials, 1968, p. 169.

22. R. Baumberger and F. Hines, "Practical Reduction Formulas for Use on Bonded Wire Straim Gages in Two-Dimensional Stress Fields," Proc. of Soc. for Exp. Stress Analysis, 2, 1, 1944, p. 113.

23. H. W. Herring, "Selected Mechanical and Physical Properties of Boron Filaments," NASA-TND-3202, National Aeronautics and Space Administration, Langley Research Center, 1966.

24. R. E. Jones, "Subroutine SMOOTH," Sandia Laboratories Mathematical Program Library, Albuquerque, New Mexico.

25. D. M. Schuster and M. Moss, "Dispersion-Strengthened Al-Al_2O_3 by Plasma Spraying," J. of Metals, 20, 1968, p. 63.

26. E. A. Block, "Dispersion-Strengthened Aluminum Alloys," Met. Revs., 6, 22, 1961, p. 193.

27. E. Orowan, Symposium on Internal Stresses in Metals and Alloys, Institute of Metals, 1948, p. 451.

28. Aluminum Standards and Data, The Aluminum Association, 1972, p. 26.

29. R. H. Ericksen, "Room Temperature Creep of Borsic-Aluminum Composites," SC-DC-714465, Sandia Laboratories, Albuquerque, New Mexico, 1972, p. 8.

30. A. H. Stang, M. Greenspan and S. B. Newman, "Poisson's Ratio of Some Structural Alloys For Large Strains," J. Res. Nat. Bureau of Stds., 37, 1946, p. 211.

31. H. L. Schreyer, private communication.

32. L. E. Malvern, Introduction to the Mechanics of a Continuous Medium, Chapter 6, Prentice-Hall, Englewood Cliffs, New Jersey, 1969.

33. Structural Design Guide for Advanced Composite Applications, Advanced Composites Division, Air Force Materials Laboratory, Wright-Patterson AFB, 1971, p. 2.2/2.1.0.

34. E. M. Lenoe, "Micromechanics of High Strength, Low Density, Boron Filament Reinforced Aluminum Metallic Composites," AFML-TR-67-125, Part I, Air Force Materials Laboratory, Wright-Patterson AFB, 1967.

35. H. G. Van Bueren, Imperfections in Crystals, Chapter 6, North-Holland Publishing Co., Amsterdam, 1960.

36. H. R. Piehler, "The Interior Elastic Stress Field in a Continuous, Close-Packed Filamentary Composite Material Under Uniaxial Tension," Fiber-Strengthened Metallic Composites, ASTM STP 427, American Society for Testing and Materials, 1967, p. 3.

37. J. M. Bloom and H. B. Wilson, "Axial Loading of a Unidirectional Composite," J. of Comp. Mat'ls, 1, 3, 1967, p. 268.

38. L. J. Ebert and J. D. Gadd, "A Mathematical Model for Mechanical Behavior of Interfaces in Composite Materials," Fiber Composite Materials, American Society for Metals, 1965, p. 89.

39. L. J. Ebert, C. H. Hamilton and S. S. Hecker, "Analytical Approach to Composite Behavior," AFML-TR-67-95, Air Force Materials Laboratory, Wright-Patterson AFB, 1967.

40. R. J. Taylor, H. Shimizu, J. F. Dolowy, et. al., "Mechanical Behavior of Aluminum-Boron Composites," AFML-TR-68-385, Air Force Materials Laboratory, Wright-Patterson AFB, 1969.

41. T. H. Lin, D. Salinas and Y. M. Ito, "Elastic-Plastic Analysis of Unidirectional Composites," J. of Comp. Mat'ls, 6, January 1972, p. 48.

42. R. H. Marloff and I. M. Daniel, "Three-Dimensional Photoelastic Analysis of a Fiber Reinforced Composite Model," Paper No. 1435, Presented to Fall Meeting Soc. Exp. Stress Analysis, San Francisco, Calif., Oct. 28-Nov. 1, 1968.

43. L. J. Ebert, R. J. Claxton, H. Kmieciak and P. K. Wright, "Analytical Approach to Composite Behavior," AFML-TR-71-133, Air Force Materials Laboratory, Wright-Patterson AFB, 1971.

TABLE 1

Plasma-Spraying Conditions Used for the Manufacture of Monolayer Tapes

Powder	- Avco 20 Aluminum (1100 alloy) - +400 -170 mesh
Gases	- arc gas - argon - 40 cfh - powder gas - argon - 25 cfh - cover gas - argon
Gun	- Plasmadyne SG-1B - electrodes - tungsten and copper - rear powder feed using a standard hopper
Power Settings	- Plasmadyne Control Panel - open circuit voltage - 80 volts - power control - 19 volts - operating voltage - 30 volts - operating current - 220 amps

Spray stand-off distance - 5 inches

TABLE 2

Nominal Chemical Analysis of 1100 Aluminum Alloy

Element	Powder %	Plasma-Sprayed %
Cu	$<<0.1$	$<<0.1$
Fe	<0.2	<0.2
Si	≈ 0.1	≈ 0.1
Mn	<0.02	<0.02
Mg	$<<0.009$	$<<0.009$
Zn	ND<0.02	ND<0.02
Ti	ND<0.009	ND<0.009
Cr	ND<0.01	ND<0.01
Ni	ND<0.01	ND<0.01
Sn	ND<0.01	ND<0.01
V	ND<0.01	ND<0.01
W	ND	ND
O	Not Analyzed	$3.61 \pm .85$

TABLE 3

Elastic and Plastic Poisson's Ratio of Borsic-Al as a Function of Filament Volume Fraction

Volume Fraction	Modulus (10^6 psi)	Elastic Poisson's Ratio	Plastic Poisson's Ratio
0	9.6	0.33	0.36
.131	15.3	0.30	0.37
.342	24.3	0.27	0.31
.409	28.1	0.26	0.32
.539	31.5	0.22	0.26

TABLE 4

Mechanical Properties of Densified Plasma-Sprayed 1100 Aluminum and Wrought 1100-0 Aluminum

	1100-0[28]	Plasma-Sprayed
Yield Strength,* psi	5,000	9,500
Ultimate Strength, psi	13,000	17,000
Elongation, percent	35	8

*0.2% offset

Figure 1. Micrograph showing the cross-sectional appearance of a 13.1 v/o 4.2 mil diameter Borsic-reinforced aluminum composite.

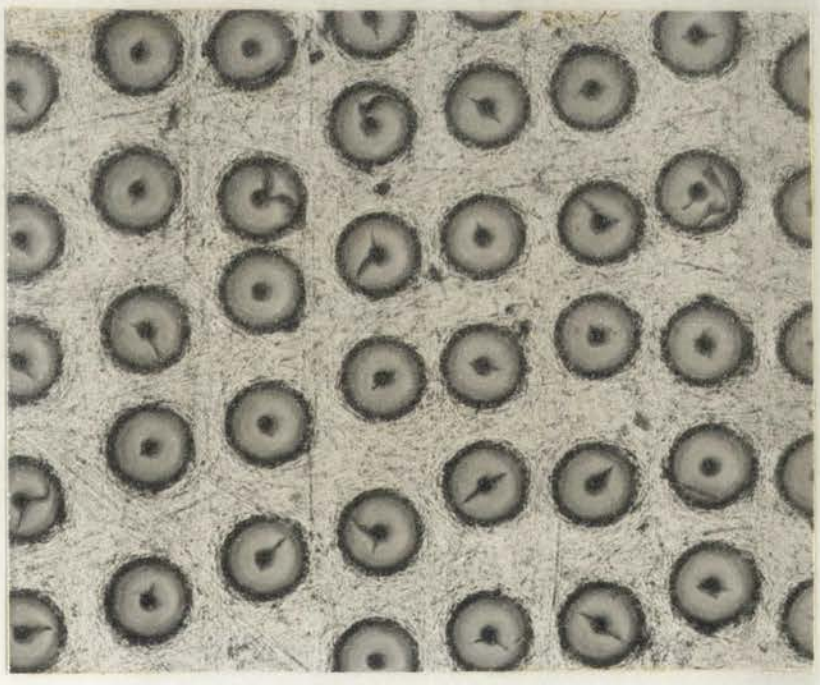

Figure 2. Micrograph showing the cross-sectional appearance of a 34.2 v/o 4.2 mil diameter Borsic-reinforced aluminum composite.

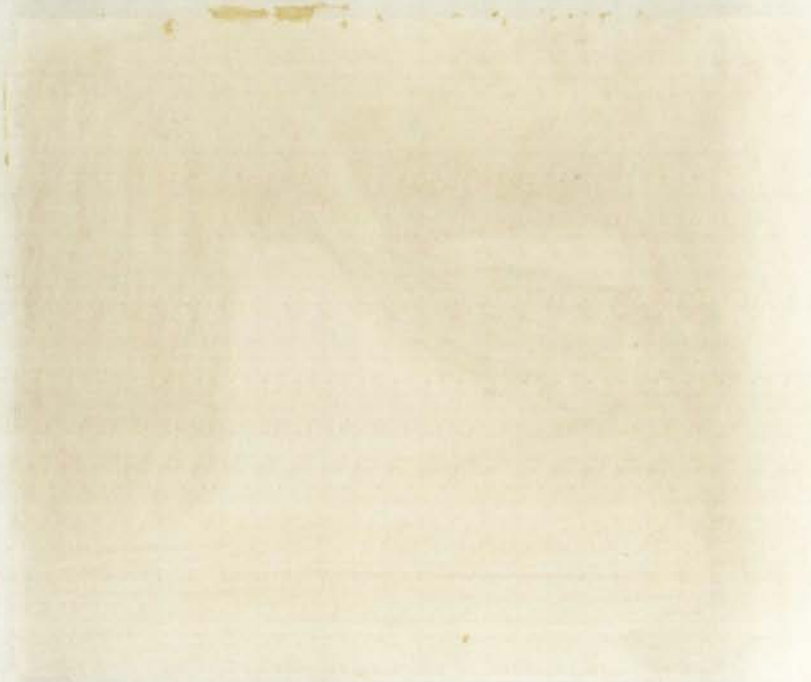

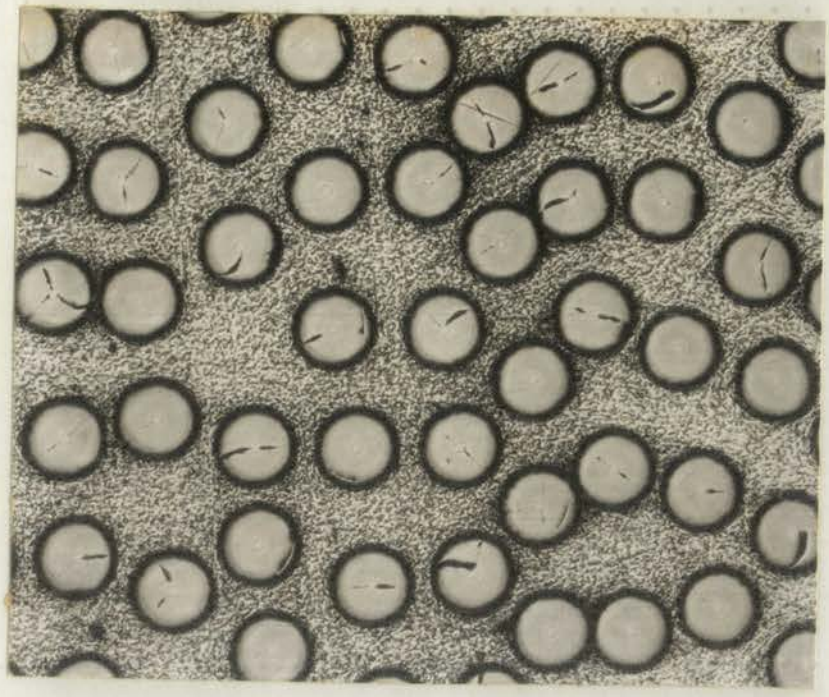

Figure 3. Micrograph showing the cross-sectional appearance of a 40.9 v/o 4.2 mil diameter Borsic-reinforced aluminum composite.

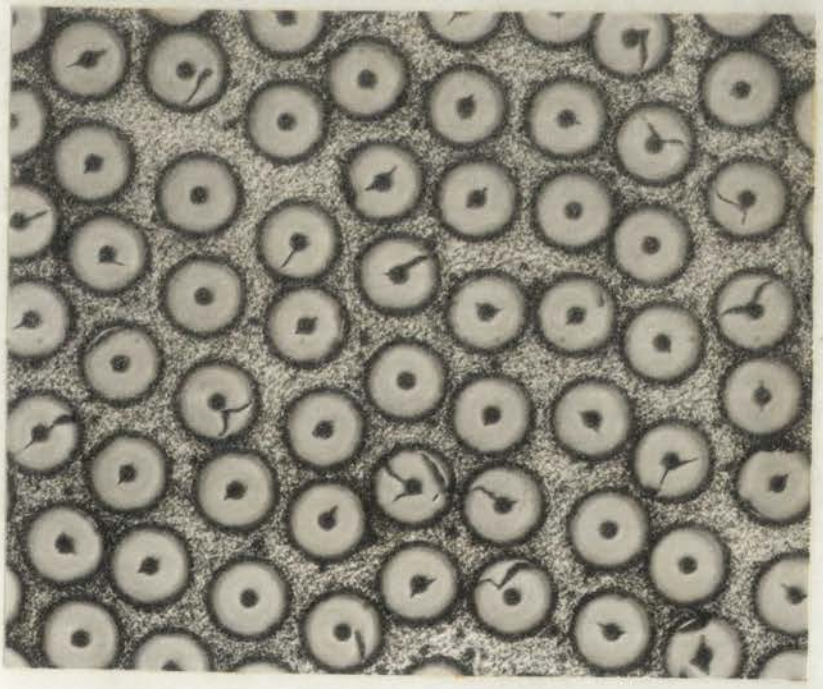

Figure 4. Micrograph showing the cross-sectional appearance of a 53.9 v/o 4.2 mil diameter Borsic-reinforced aluminum composite.

Figure 5. Micrograph showing the cross-sectional appearance of densified plasma-sprayed 1100 aluminum, 250X.

Figure 6. Micrograph showing the cross-sectional appearance of densified plasma-sprayed 1100 aluminum, etched, 250X.

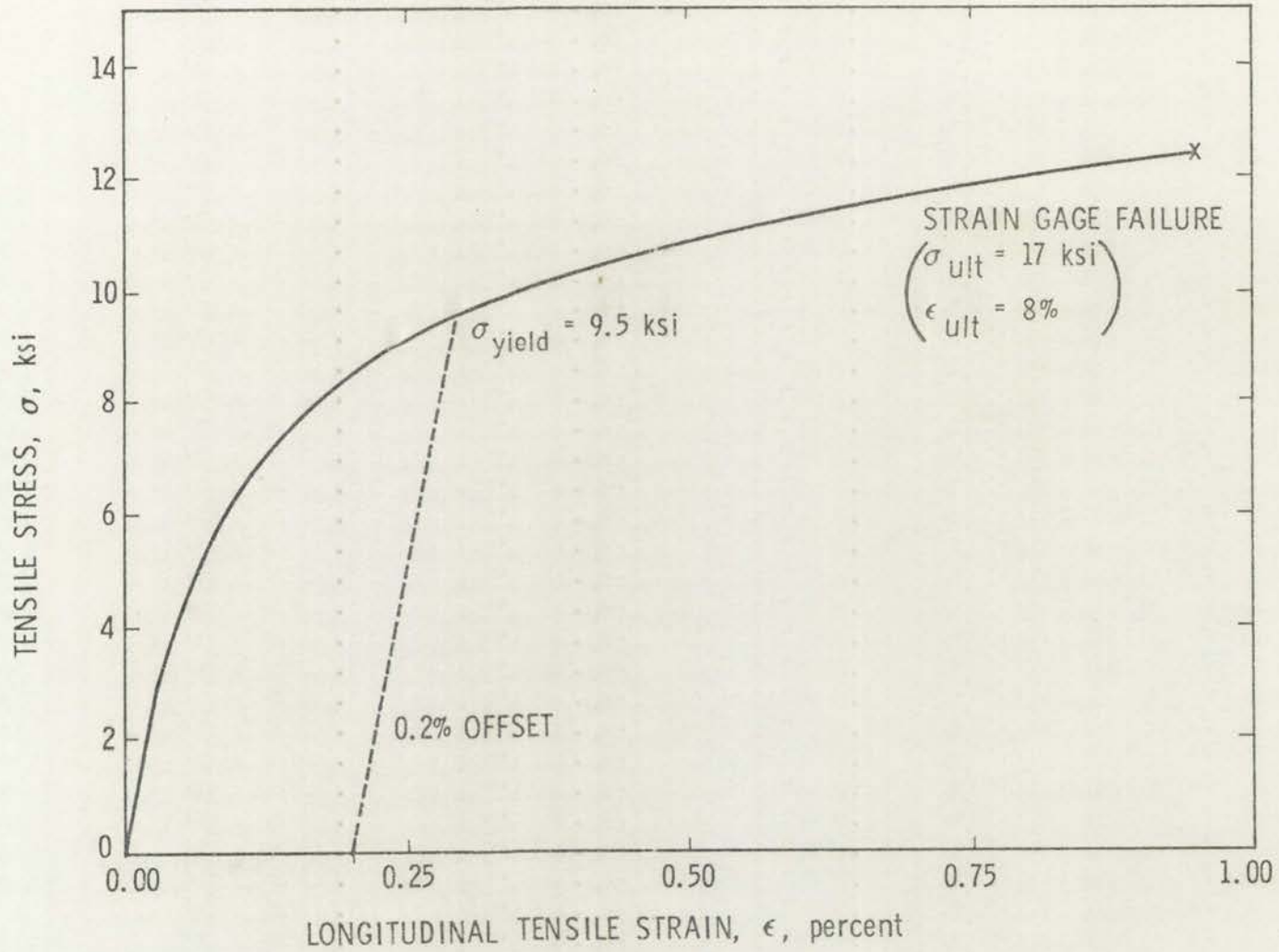

Figure 7. Stress versus strain curve of densified plasma-sprayed 1100 aluminum alloy.

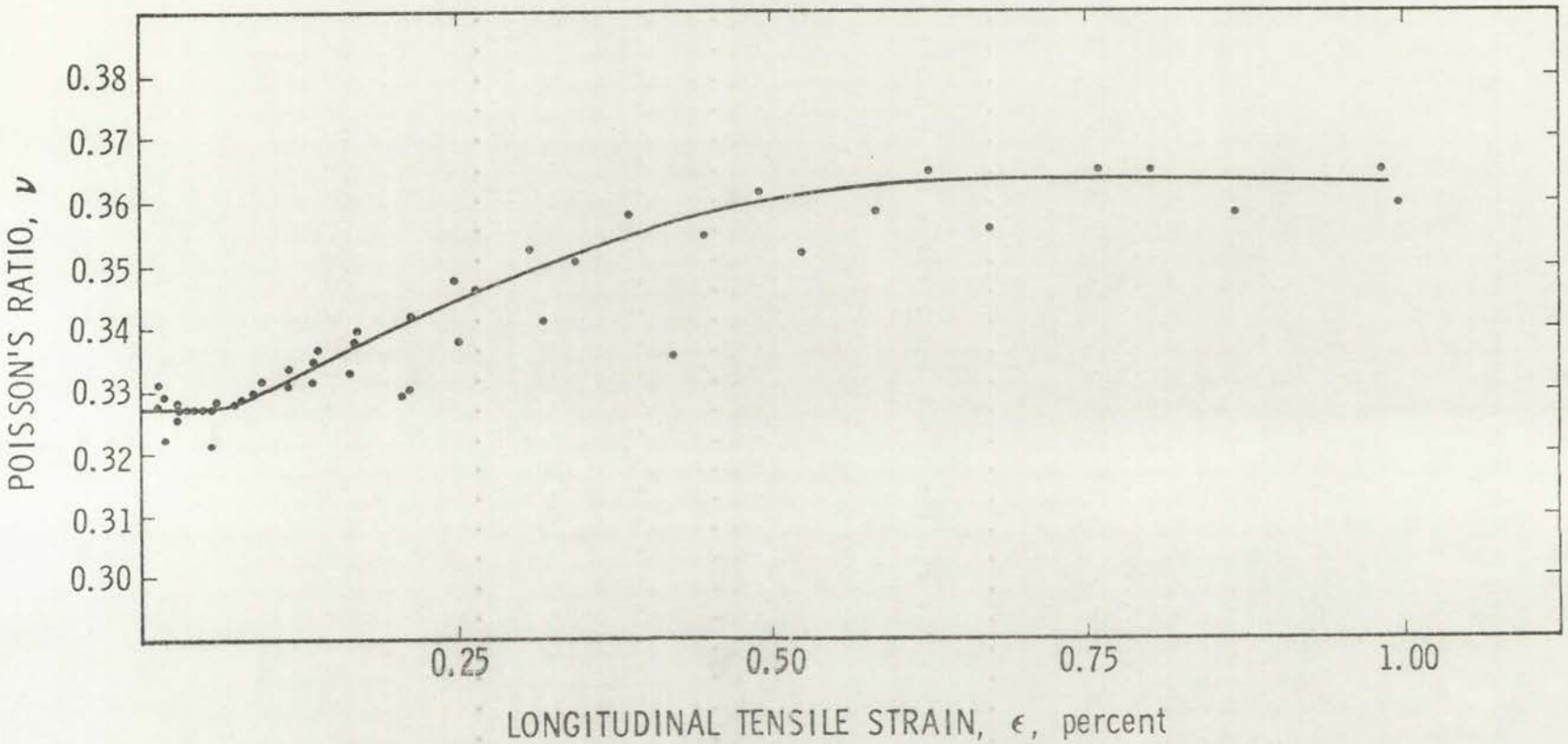

Figure 8. Poisson's ratio versus strain for densified plasma-sprayed 1100 aluminum alloy.

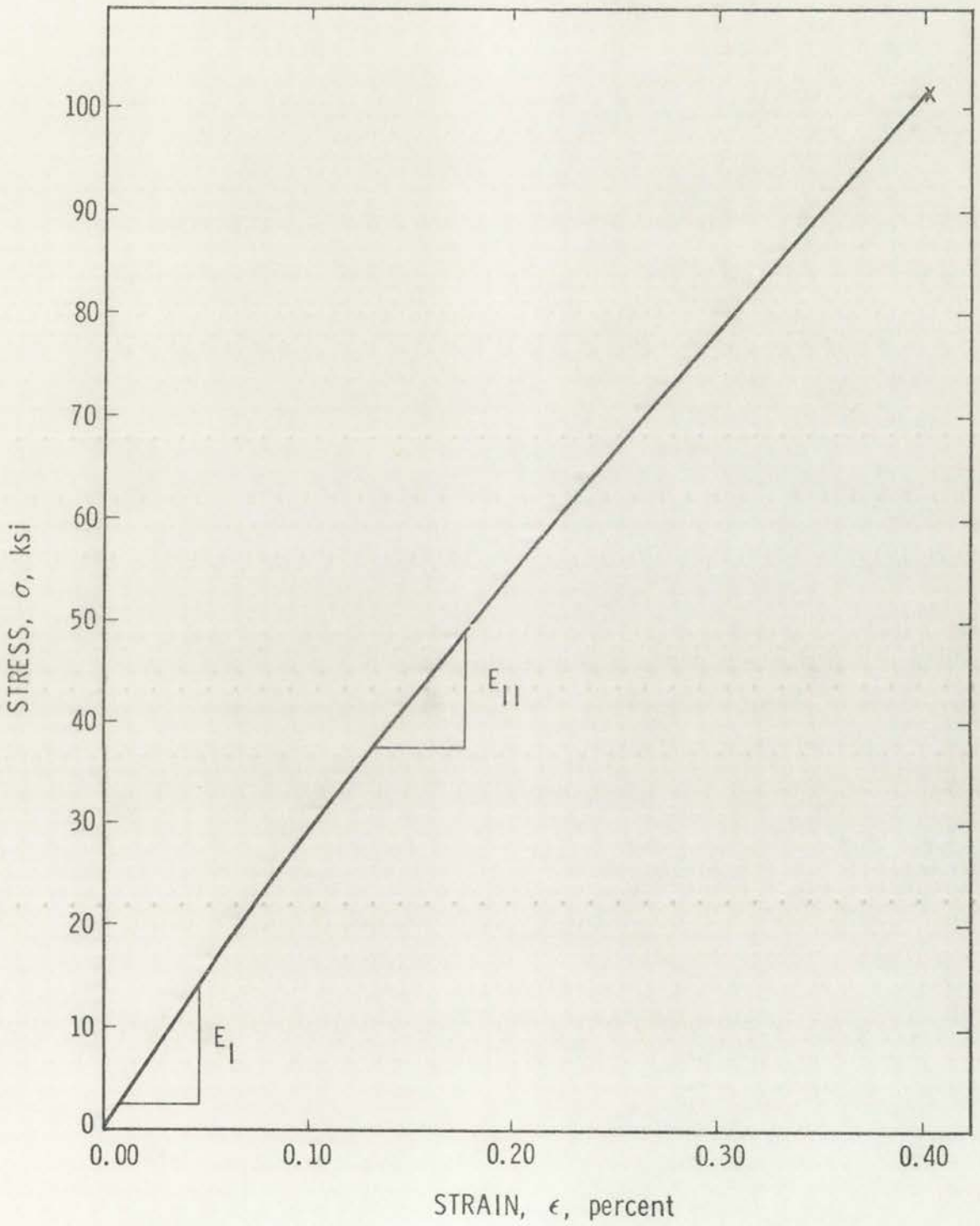

Figure 9. Stress versus strain curve for 53.9 volume percent Borsic-aluminum composite.

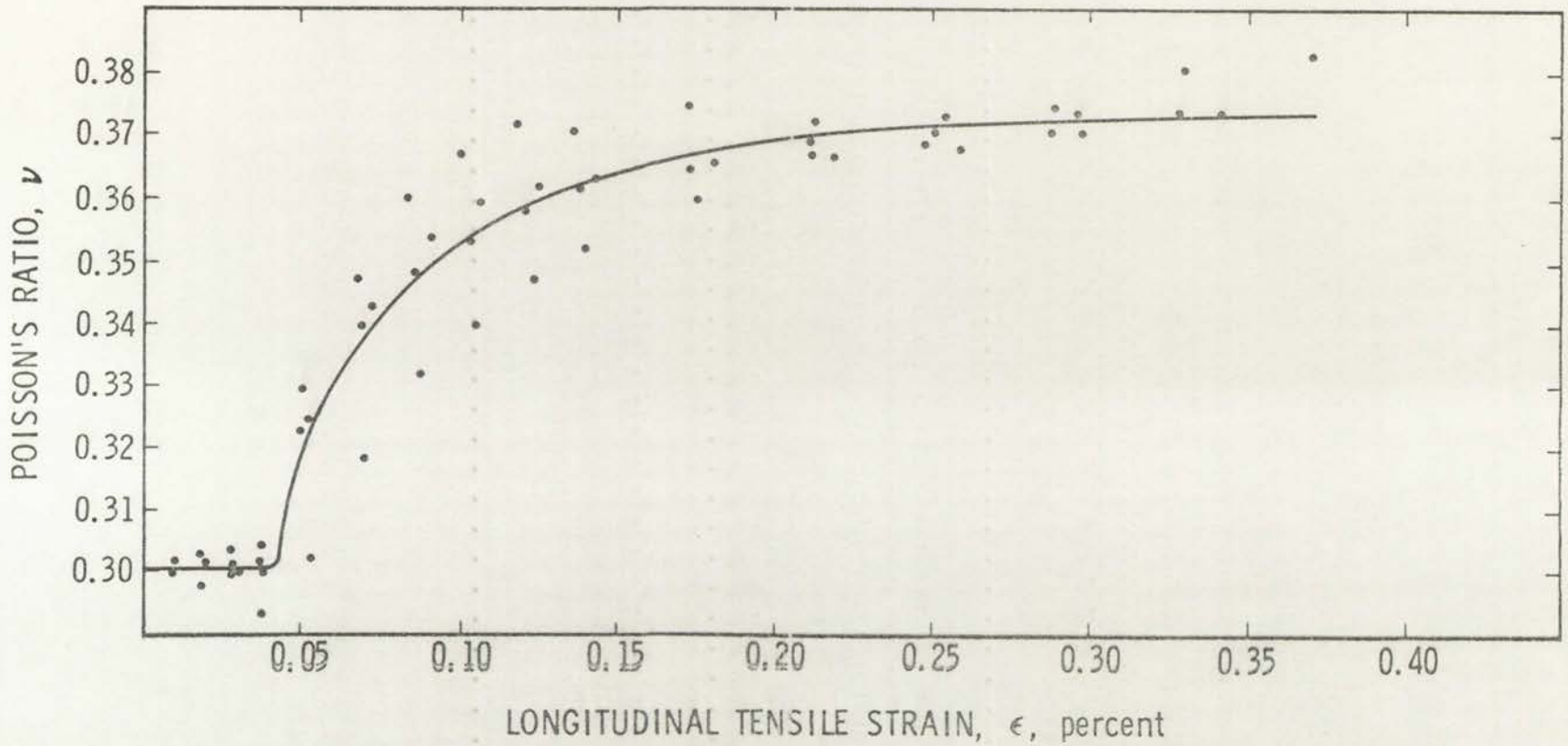

Figure 10. Poisson's ratio as a function of strain for a 13.1 v/o Borsic-aluminum composite.

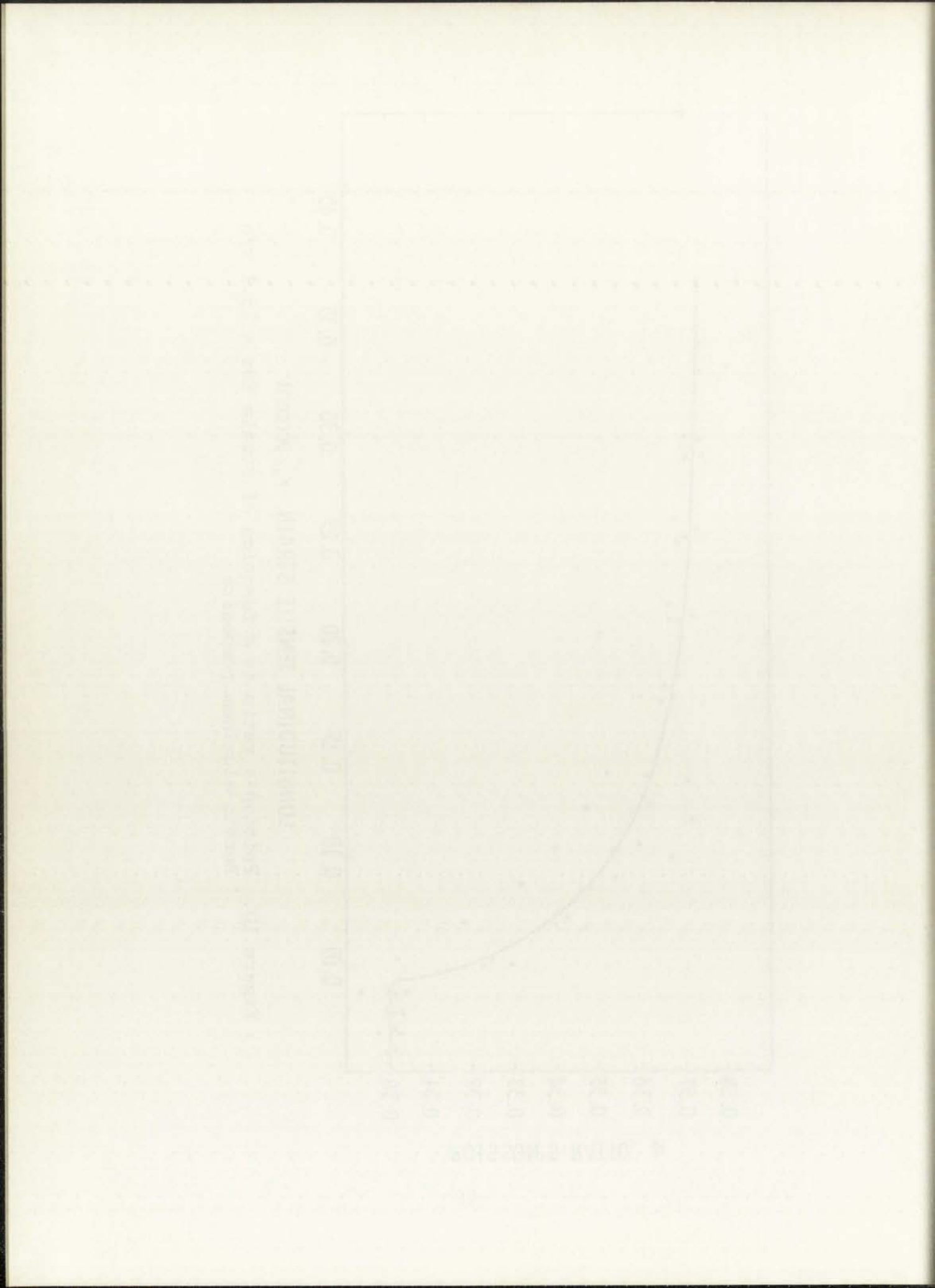

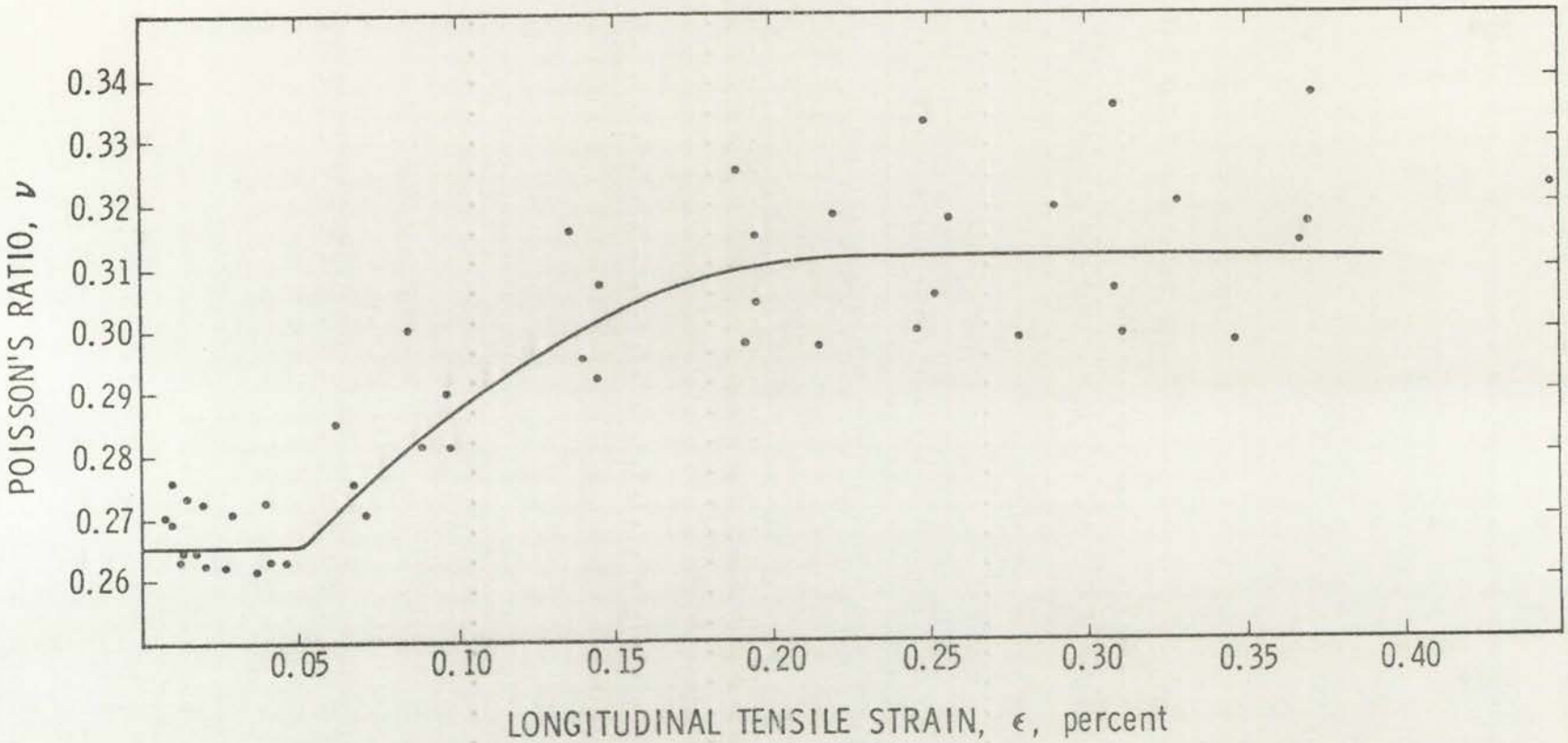

Figure 11. Poisson's ratio as a function of strain for a 34.2 v/o Borsic-aluminum composite.

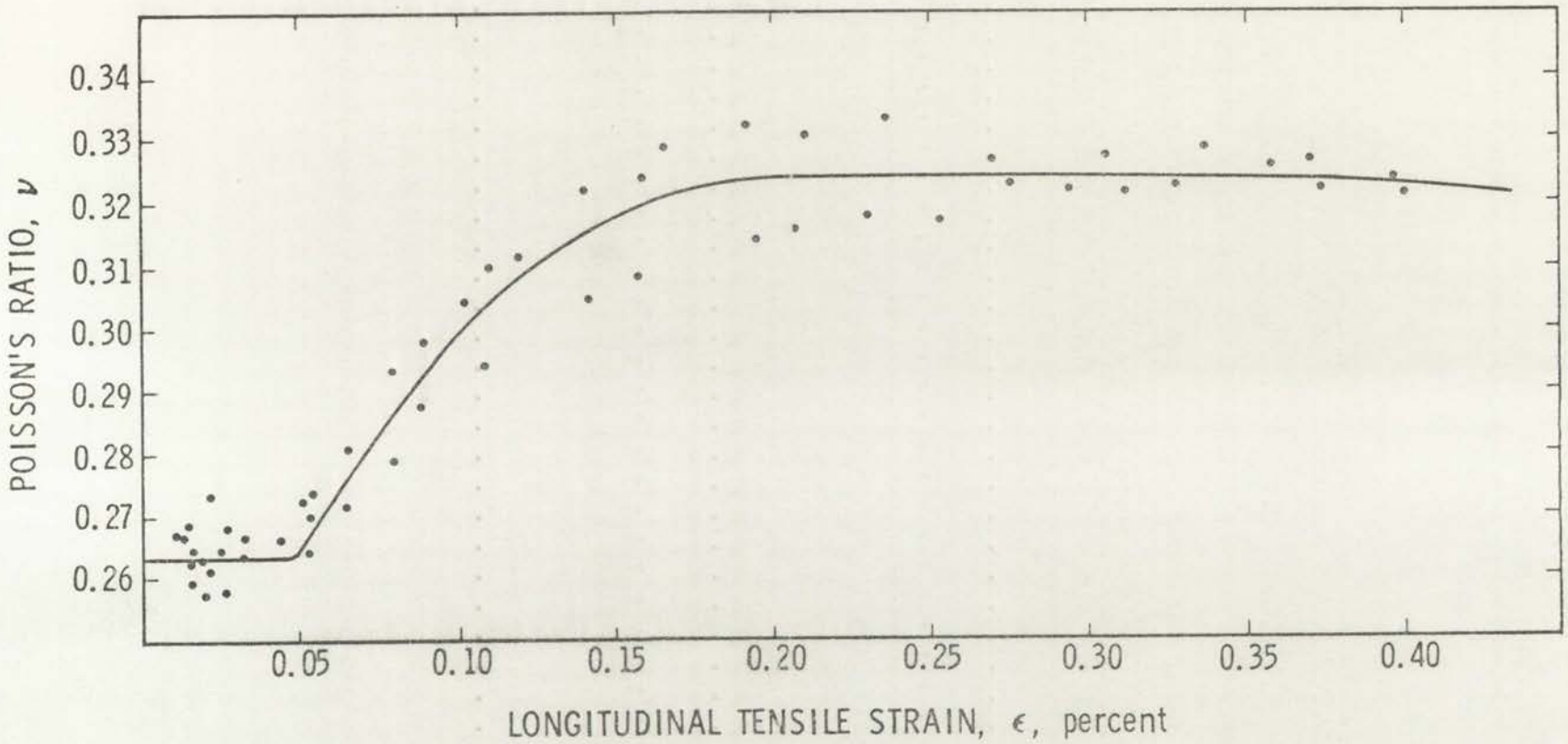

Figure 12. Poisson's ratio as a function of strain for a 40.9 v/o Borsic-aluminum composite.

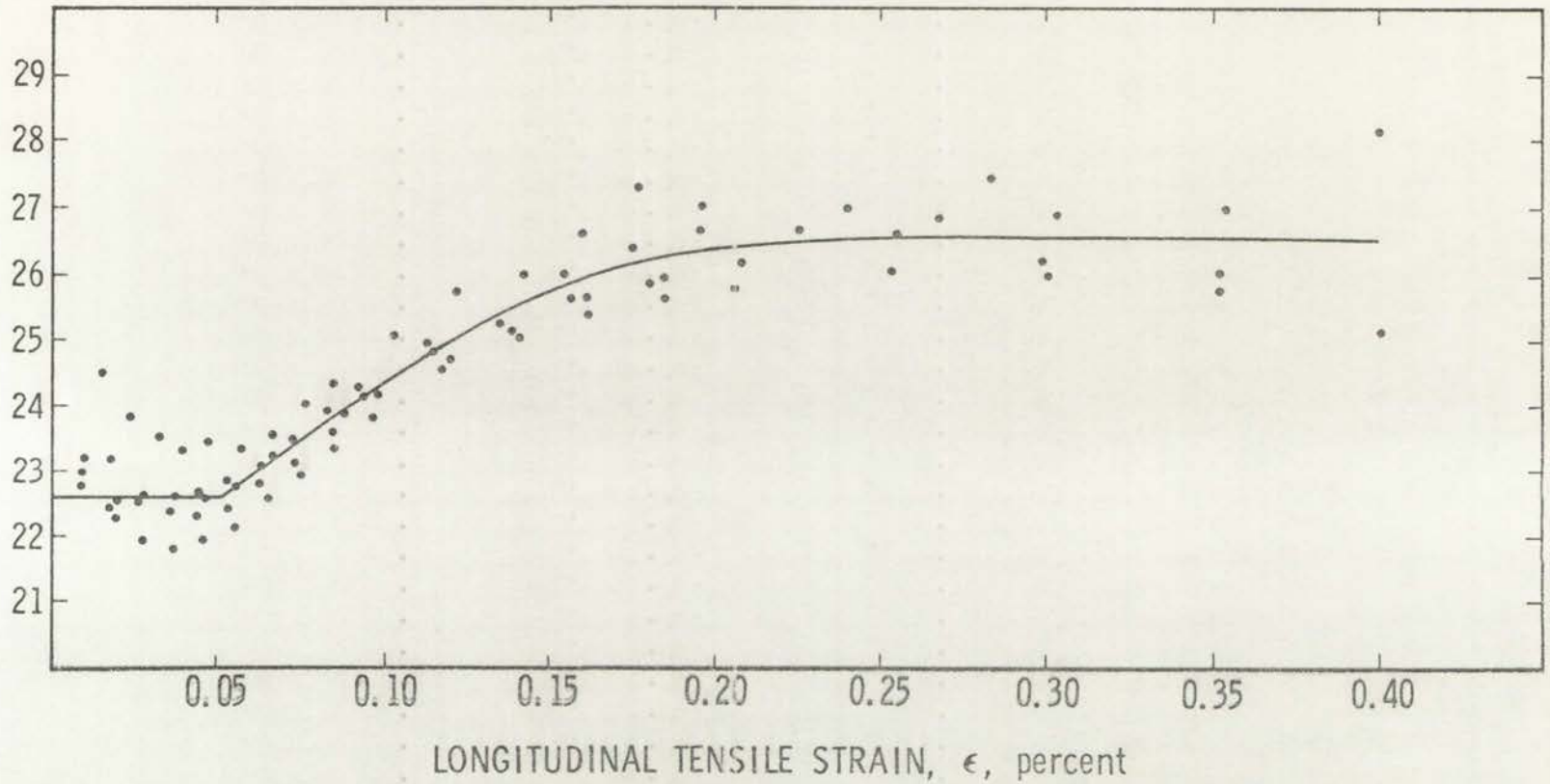

Figure 13. Poisson's ratio as a function of strain for a 53.9 v/o Borsic-aluminum composite.

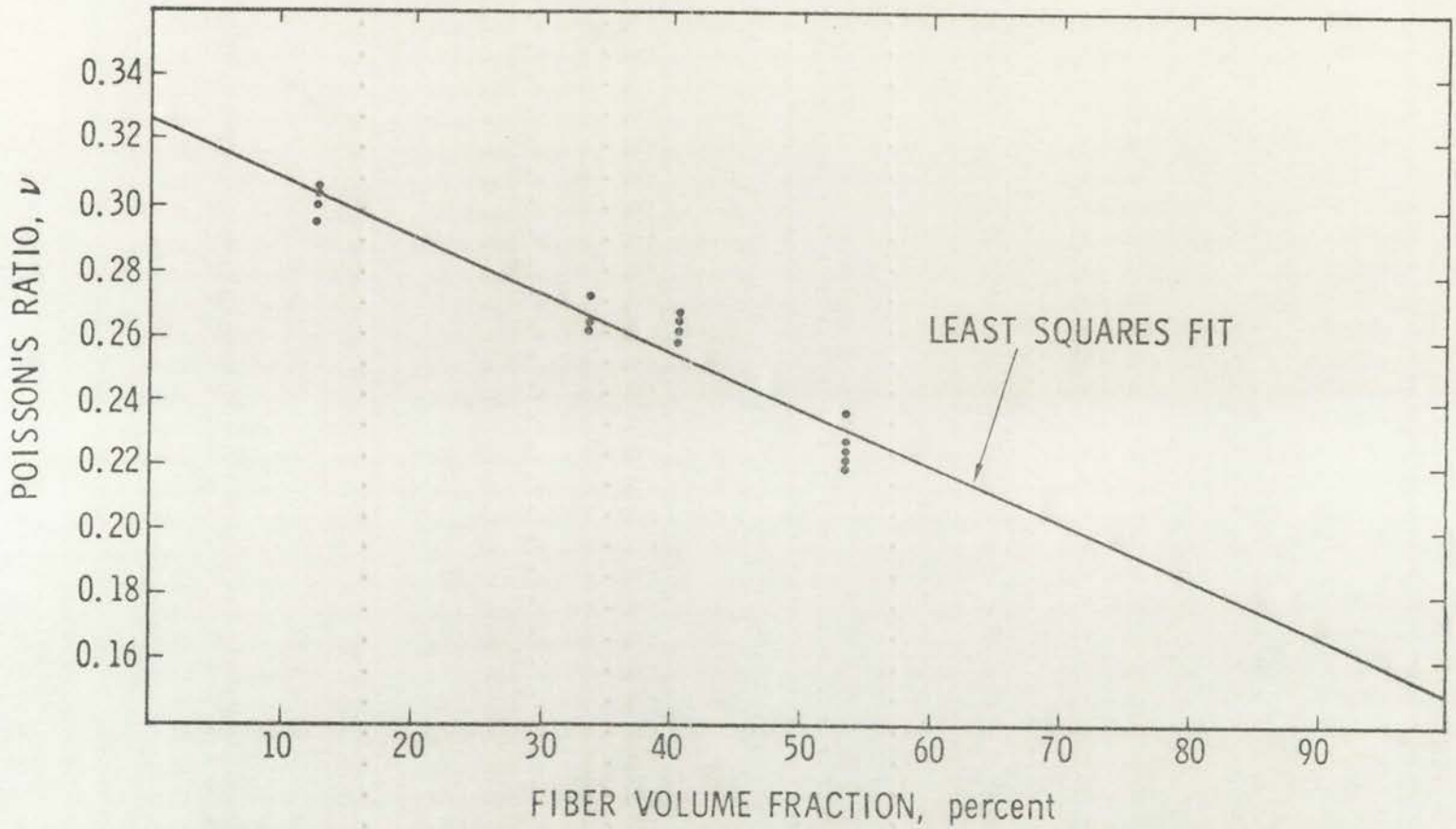

Figure 14. Elastic Poisson's ratio versus v/o Borsic for Borsic-reinforced aluminum composite.

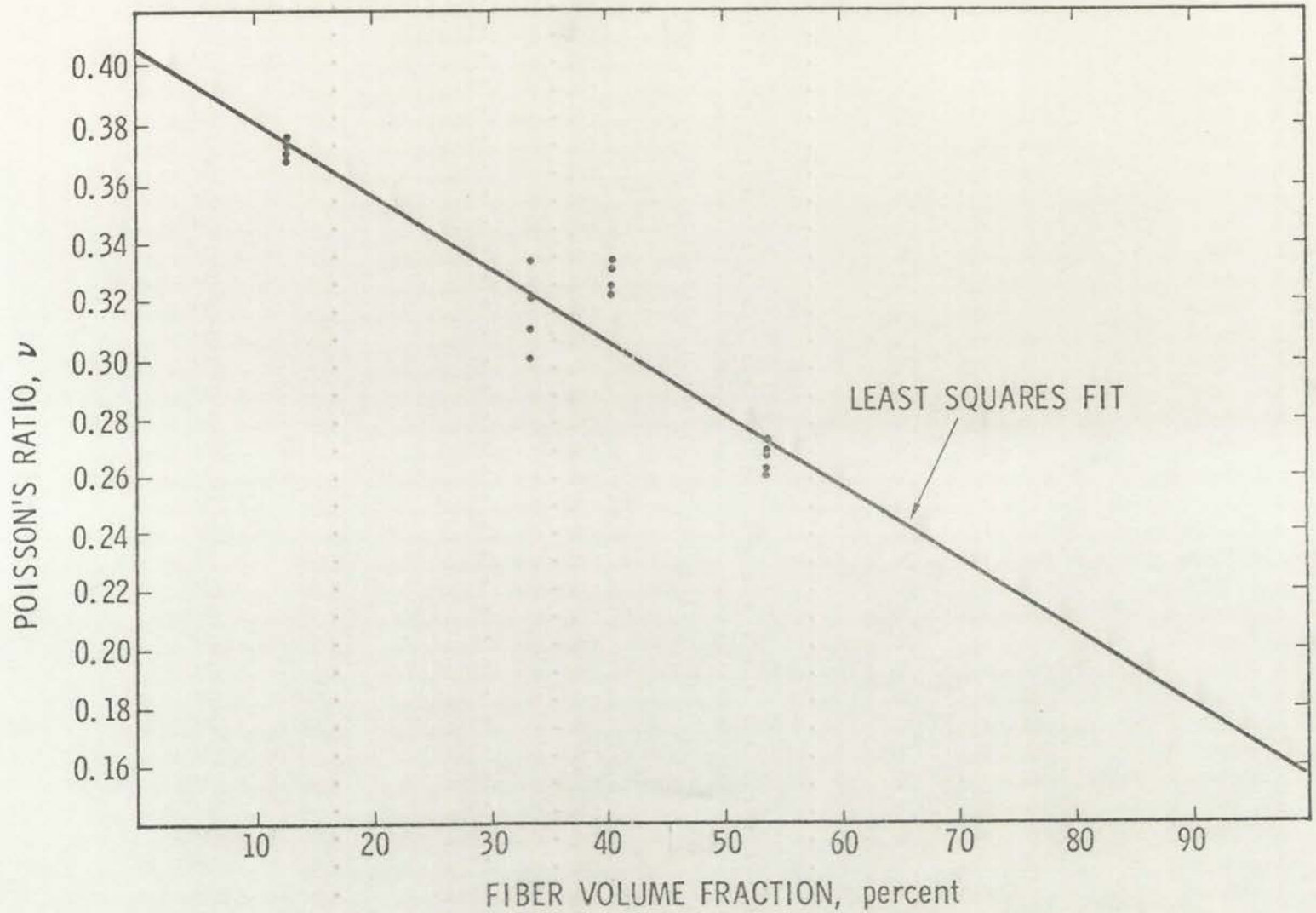

Figure 15. Plastic Poisson's ratio versus v/o Borsic for Borsic-reinforced aluminum composites.